ORIGINAL ARTICLE

Prostate Cancer

The applied research of simultaneous image acquisition of T2-weighted imaging (T2WI) and diffusion-weighted imaging (DWI) in the assessment of patients with prostate cancer

Yi Liu*, Wei Wang*, Xiu-Bo Qin, Hui-Hui Wang, Ge Gao, Xiao-Dong Zhang, Xiao-Ying Wang

We aimed to evaluate the feasibility of simultaneous image acquisition of multiple instantaneous switchable scan (MISS) for prostate magnetic resonance imaging (MRI) on 3T. Fifty-three patients were scanned with MRI due to suspected prostate cancer. Twenty-eight of them got histological results. First, two readers assessed the structure delineation and image quality based on images of conventional T2-weighted imaging (T2WI) and diffusion-weighted imaging (DWI) (CTD). Second, two readers identified the index lesion together, and then, reader one evaluated the contrast of index lesion on T2WI and signal ratio on apparent diffusion coefficient map. Third, they assigned Prostate Imaging Reporting and Data System (PI-RADS) score in consensus for the index lesion. After 4 weeks, the images of MISS were reviewed by the same readers following the same process. Finally, two readers gave preference for image interpretation, respectively. Kappa coefficient, Wilcoxon signed-rank test, paired-sample t-test, Bland–Altman analysis, and receiver operating characteristic (ROC) analysis were used for statistical analysis. The acquisition time of CTD was 6 min and 10 s, while the acquisition time of MISS was 4 min and 30 s. Interobserver agreements for image evaluation were $\kappa = 0.65$ and $\kappa = 0.80$ for CTD and MISS, respectively. MISS-T2WI showed better delineation for seminal vesicles than CTD-T2WI (reader 1: $P < 0.001$, reader 2: $P = 0.001$). The index lesion demonstrated higher contrast in MISS-T2WI ($P < 0.001$). The PI-RADS scores based on CTD and MISS exhibited high ability in predicting clinically significant cancer (area under curve [AUC] = 0.828 vs 0.854). Readers preferred to use MISS in 41.5%–47.2% of cases. MISS showed comparable performance to conventional technique with less acquisition time.

INTRODUCTION

Multiparametric magnetic resonance imaging (mpMRI) is becoming increasingly important in the workup of prostate cancer (PCa).[1,2] A combination of anatomical MRI (*e.g.*, T2-weighted imaging [T2WI]) and functional imaging such as diffusion-weighted imaging (DWI) and dynamic contrast-enhanced MRI (DCE-MRI) is effective for the detection of clinically significant PCa. The Prostate Imaging Reporting and Data System version 2 (PI-RADS v2)[3] has been proposed for the assessment of prostate lesions on T2WI, DWI, and DCE-MRI. According to the PI-RADS v2 system, T2WI and DWI are considered to be the dominant imaging sequences for identifying clinically significant PCa, whereas the added value provided by DCE-MRI appears to be modest.[4] The diagnostic performance of T2WI and DWI in combination is not inferior to mpMRI and thereby offers a valid option for reducing examination cost and time.[5] It therefore seems reasonable that some researchers suggest using a biparametric prostate MRI protocol that incorporates T2WI and DWI but leaves out DCE.[6] Furthermore, with the recently developed MRI technique of multiple instantaneous switchable scan (MISS),[7,8] both three-dimensional (3D) T2WI and 2D DWI can be acquired simultaneously during one repetition time.

The purpose of this preliminary study was therefore to evaluate the feasibility of MISS on 3T MRI, comparing the image quality and diagnostic efficacy of images acquired using a MISS sequence with those acquired using conventional 2D T2WI and 2D DWI (CTD).

PARTICIPANTS AND METHODS

Study participants

This study was conducted at Peking University First Hospital (Beijing, China). The study protocol was approved by the Institutional Review Board of the Peking University First Hospital, with a waiver for the requirement for informed consent as this study was a retrospective study.

Clinical and imaging data were collected from 53 consecutive patients (age, mean ± standard deviation [s.d.]: 66.0 ± 11.3 years, range: 24–84 years) who underwent an mpMRI examination between November 2015 and April 2016 because of suspected prostate disease. All the patients met the following inclusion criteria: prostate-specific antigen >4.4 ng ml^{-1}; no previous treatment of the prostate gland (such as operation, medication, or radiation therapy) before MRI scanning; and images were available for evaluation. Histologic results

were available for 28 patients after the MRI examination, while no pathological findings were available for the other 25 patients during the 3 months following the MRI examination.

Magnetic resonance imaging protocol

The mpMRI examinations were performed on a 3T scanner (Achieva TX, Philips, Best, The Netherlands) with a 32-channel phased-array coil.[9] In all patients, the sequences were performed in the following order: T1WI, CTD, MISS, and DCE. The same imaging coordinates were used for the CTD and MISS imaging. The detailed scan parameters for these sequences were presented in **Table 1**. The acquisition time for the CTD was 6 min and 10 s, while the acquisition time for the MISS was 4 min and 30 s.

In this study, the MISS technique describes an interleaved scanning method involving the simultaneous acquisition of 3D T2WI and 2D DWI. Each shot of the DWI scan was interleaved in the duration between the two repeated cycles of the 3D T2WI scan, so that the 3D T2WI and 2D DWI could be sampled simultaneously during one repetition time.

Imaging analyses

The prostate MRI images were retrospectively interpreted by two experienced radiologists (WW [reader 1] was a radiology resident with 5 years of experience in prostatic and oncological imaging and XYW [reader 2] was a staff radiologist with 20 years of experience in prostatic and oncological imaging) on the Picture Archiving and Communication System (PACS) of the radiology department. The two readers were blinded to the clinical information and pathological results.

The two radiologists were asked to independently grade the CTD images using a 3-point scoring system (1, not clearly defined; 2, moderately defined; and 3, clearly defined), in terms of the presence of delineation of the prostate zonal anatomy, prostate capsule, nerve vascular bundle, and seminal vesicles. The image quality of each CTD sequence was also scored by the two readers with regard to sharpness, contrast, deformation, and image artifact (1, poor image quality for diagnosis, not interpretable; 2, evident distortion, limited detail or delineation of lesions with surrounding tissue, acceptable image quality for diagnosis; and 3, excellent image quality for confident diagnosis and sharply defined borders, no distortion).

The two readers identified the index lesion together. Reader 1 was asked to measure and calculate the relative contrast of the index lesion on T2WI and its signal ratio on an apparent diffusion coefficient (ADC) map, according to previously described methods.[10–12] This procedure was used to provide a rough estimate of the relative signal contrast, irrespective of the overall image noise, and to eliminate the effect of signal differences between the different sequences.[13] The relative contrast of the index lesion and the signal ratio were calculated according to the following equations: relative contrast of index lesion = $(SI_{Normal} - SI_{Lesion})/(SI_{Normal} + SI_{Lesion})$, where SI is the signal intensity, and signal ratio = $ADC_{Lesion}/ADC_{Normal}$. A region of interest (ROI) was

drawn in the index lesion and in a normal-appearing corresponding area of the prostate. For each patient, the ROIs were fixed at the same size (3–10 mm²) and were drawn at the same level in the CTD images.

PI-RADS scores were assigned for each individual patient according to the index lesions on CTD,[14] with the two readers giving the PI-RADS scores for each individual patient independently at the same time. If there were discrepancies between the two readers, a consensus was obtained through discussion. After a period of 4 weeks to avoid any recall bias from the CTD assessment, the same readers evaluated the MISS acquisitions following the same process. For each patient, the ROIs of the MISS images were drawn at the same level as those of the CTD images. One reader then compared the subjective and objective evaluations of the CTD with those of the MISS and evaluated the diagnostic efficacy of the PI-RADS scores based on CTD with those based on MISS.

The two readers were also asked to state their preference between MISS and CTD using a 3-point scale (1, prefer CTD; 2, no preference; and 3, prefer MISS). This preference was determined according to the following criteria: comparison of structural display, imaging quality, and contrast of the index lesion, according to the reader's subjective feelings.

Histopathologic correlation

For 28 patients, histopathologic results (*n* = 28) were obtained by ultrasound-guided systematic and targeted biopsy within the 3 months following the MRI examination. Transrectal ultrasound-guided systematic biopsies using needles of ≥6-core (usually 12- or 13-core needles) plus targeted biopsies of any area suspicious for malignancy were performed in all 28 patients by urologists in the operating room. All biopsy specimens were evaluated by a dedicated genitourinary pathologist to determine the presence of PCa, with the Gleason score being determined in positive cases. There were 12 cases of clinically significant PCa (Gleason score ≥7), 3 cases of nonsignificant cancer (Gleason score = 6), 1 prostatic intraepithelial neoplasia, 6 chronic prostatitis, 1 benign prostatic hyperplasia, 4 prostate tissue with absence of gland basal cell, and 1 seminal vesicle schwannoma. The diagnostic efficacy of the CTD and MISS MRI images of the 28 patients was evaluated against the histopathology results, which were considered the gold standard.

Statistical analyses

All statistical analyses were performed using SPSS version 20.0 (IBM Corp., Armonk, NY, USA). Data from 53 patients were used to compare structure delineation and image quality, lesion contrast, and preference choice. Data from the 28 patients for whom histological results were available were used for comparisons of diagnostic efficacy. A kappa coefficient was used to assess agreement between the observers, with a value of $\kappa \geq 0.60$ being considered to indicate good interobserver agreement. $P < 0.05$ was considered statistically significant. As variables were described in the form of count data,

Table 1: Summary of imaging parameters for sequences applied for magnetic resonance imaging scans

Imaging parameter	T1WI	CTD-T2WI	CTD-DWI	MISS-T2WI	MISS-DWI	DCE
TR (ms)	567	2900	4000	1500	4000	3.3
TE (ms)	10	90	70	100	70	1.59
Matrix size (dots per FOV)	236×354	320×280	184×184	240×201	184×184	256×256
FOV (mm × mm)	200×302	240×240	260×260	120×180	260×260	311×302
Flip angles (°)	90	90	90	90	90	15
b (s mm⁻²)	NA	NA	1000	NA	1000	NA
Thickness (mm)	4	4	4	1	4	2.5

T1WI: T1-weighted imaging; T2WI: T2-weighted imaging; DWI: diffusion-weighted imaging; DCE: dynamic contrast enhanced; CTD: conventional 2D T2WI and 2D DWI; MISS: multiple instantaneous switchable scan; TR: repetition time; TE: echo time; FOV: field of view; *b*: diffusion sensitivity coefficient; NA: not applicable

the Wilcoxon signed-rank test was used to determine differences in structure delineation and image quality between MISS and CTD. Paired-sample *t*-tests were used to assess the difference in the contrast of index lesion between MISS-T2WI and CTD-T2WI and between MISS-ADC maps and CTD-ADC maps. Bland–Altman analysis was implemented using GraphPad Prism 6.0 (GraphPad Software Corp., San Diego, CA, USA), to validate the differences between PI-RADS scores based on MISS images and those based on CTD images. Receiver operating characteristic (ROC) curves were generated to illustrate the predictive accuracy of the PI-RADS score for clinically significant PCa.

RESULTS

Subjective evaluation of structure delineation and image quality

The interobserver reproducibility was substantial for the subjective image evaluation, both for the CTD (κ = 0.65) and for the MISS (κ = 0.80).

The CTD-T2WI, CTD-DWI, MISS-T2WI, and MISS-DWI were all rated as having clear structure delineation (a score of 3). The MISS-T2WI scored higher than the CTD-T2WI for delineation of the fine structure of seminal vesicles (reader 1, CTD-T2WI: 67.9% [36/53] *vs* MISS-T2WI: 98.1% [52/53], $P < 0.001$; reader 2: 62.3% [33/53] *vs* 90.6% [48/53], $P = 0.001$; **Figure 1**, **Table 2** and **3**). There were no evident differences in the delineation of prostate zonal anatomy, prostate capsule, nerve vascular bundle, and image quality between MISS-T2WI and CTD-T2WI (**Table 2** and **3**). There were also no evident differences in structure delineation and image quality between MISS-DWI and CTD-DWI (**Table 4** and **5**).

Objective evaluation of lesion contrast on T2WI and DWI

For the index lesion of each patient, the contrast ratio on MISS-T2WI was higher than that on CTD-T2WI (mean ± s.d.: MISS-T2WI: 0.27 ± 0.12 *vs* CTD-T2WI: 0.21 ± 0.13; $P < 0.001$; **Figure 1**). Out of all 53 cases, 32 lesions were in the peripheral zone (PZ), 19 lesions were in the transitional zone (TZ), 1 lesion surrounded the urethra, and 1 case was without any lesion. MISS-T2WI showed a higher contrast ratio for the lesions, both in the PZ (mean ± s.d.: 0.27 ± 0.15 *vs* 0.21 ± 0.16; $P < 0.001$) and the TZ (mean ± s.d.: 0.18 ± 0.09 *vs* 0.22

± 0.07; $P = 0.010$). The signal ratio of the MISS-ADC maps was not significantly different to that of the CTD-ADC maps (mean ± s.d.: 0.56 ± 0.15 *vs* 0.57 ± 0.16; $P = 0.740$).

Diagnostic efficacy with PI-RADS score

Bland–Altman plots were used to evaluate differences between the PI-RADS scores based on CTD and those based on MISS. These
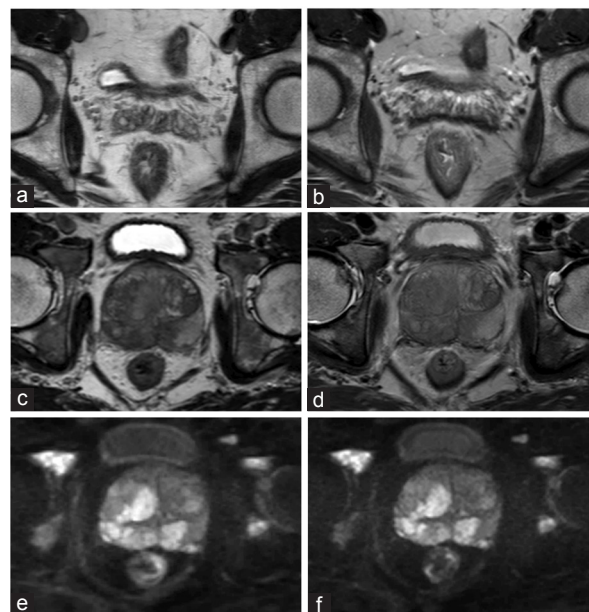

Figure 1: (**a**) The image of MISS-T2WI of a 52-year-old man with prostate cancer. (**b**) The image of conventional T2WI of the same patient. The two figures showed the seminal vesicles delineation was better in MISS-T2WI than the conventional sequence. (**c**) 3D-T2WI in MISS of a 66-year-old man with prostate cancer. (**d**) 2D-T2WI in conventional T2WI of the same patient. The lesion showed slightly better lesion contrast on MISS-T2WI than the conventional T2WI. (**e**) DWI in MISS. (**f**) Conventional DWI. There was no obvious difference of image quality between MISS-DWI and conventional DWI. MISS: multiple instantaneous switchable scan; T2WI: T2-weighted imaging; 3D: three-dimensional; DWI: diffusion-weighted imaging.

Table 2: Structure delineation and image quality comparison between CTD-T2-weighted imaging and multiple instantaneous switchable scan-T2-weighted imaging by reader 1

Content	Sequences	Score of 3	Score of 2	Score of 1	Ratio of clearly structure delineation (%)	Z	P
Delineation of structure							
Zonal anatomy	CTD-T2WI	52	1	0	98.1	−0.577	0.564
	MISS-T2WI	51	2	0	96.3		
Prostate capsule	CTD-T2WI	49	4	0	92.5	−0.378	0.705
	MISS-T2WI	48	5	0	90.6		
Nerve vascular bundle	CTD-T2WI	41	12	0	77.4	−1.500	0.134
	MISS-T2WI	48	4	1	90.6		
Seminal vesicles	CTD-T2WI	36	16	1	67.9	−3.770	0.000
	MISS-T2WI	52	1	0	98.1		
Image quality							
Sharpness	CTD-T2WI	53	0	0	100	−1.000	0.317
	MISS-T2WI	52	1	0	98.1		
Contrast	CTD-T2WI	53	0	0	100	0	1.000
	MISS-T2WI	53	0	0	100		
Deformation	CTD-T2WI	53	0	0	100	0	1.000
	MISS-T2WI	53	0	0	100		
Artifact	CTD-T2WI	49	4	0	92.5	−0.816	0.414
	MISS-T2WI	51	2	0	96.3		

CTD: conventional 2D T2WI and 2D DWI; MISS: multiple instantaneous switchable scan; T2WI: T2-weighted imaging; DWI: diffusion-weighted imaging

Table 3: Structure delineation and image quality comparison between CTD-T2-weighted imaging and multiple instantaneous switchable scan-T2-weighted imaging by reader 2

Content	Sequences	Score of 3	Score of 2	Score of 1	Ratio of clearly structure delineation (%)	Z	P
Delineation of structure							
Zonal anatomy	CTD-T2WI	47	6	0	88.7	−1.000	0.317
	MISS-T2WI	49	4	0	92.5		
Prostate capsule	CTD-T2WI	50	3	0	94.3	−1.000	0.317
	MISS-T2WI	51	2	0	96.3		
Nerve vascular bundle	CTD-T2WI	45	8	0	84.9	−1.897	0.058
	MISS-T2WI	51	1	1	96.3		
Seminal vesicles	CTD-T2WI	33	19	1	62.3	−3.441	0.001
	MISS-T2WI	48	4	1	90.6		
Image quality							
Sharpness	CTD-T2WI	49	4	0	92.5	−1.000	0.317
	MISS-T2WI	51	2	0	96.3		
Contrast	CTD-T2WI	52	1	0	98.1	−1.000	0.317
	MISS-T2WI	53	0	0	100		
Deformation	CTD-T2WI	53	0	0	100	0	1.000
	MISS-T2WI	53	0	0	100		
Artifact	CTD-T2WI	46	7	0	86.8	−0.378	0.705
	MISS-T2WI	47	6	0	88.7		

CTD: conventional 2D T2WI and 2D DWI; MISS: multiple instantaneous switchable scan; T2WI: T2-weighted imaging; DWI: diffusion-weighted imaging

Table 4: Structure delineation and image quality comparison between CTD-diffusion-weighted imaging and multiple instantaneous switchable scan-diffusion-weighted imaging by reader 1

Content	Sequences	Score of 3	Score of 2	Score of 1	Ratio of clearly structure delineation (%)	Z	P
Delineation of structure							
Zonal anatomy	CTD-DWI	50	3	0	94.3	0	1.000
	MISS-DWI	50	3	0	94.3		
Prostate capsule	CTD-DWI	49	4	0	92.5	−1.414	0.157
	MISS-DWI	51	2	0	96.3		
Nerve vascular bundle	CTD-DWI	45	8	0	84.9	−1.000	0.317
	MISS-DWI	44	9	1	83.0		
Seminal vesicles	CTD-DWI	45	8	0	84.9	0	1.000
	MISS-DWI	45	8	0	84.9		
Image quality							
Sharpness	CTD-DWI	45	8	0	84.9	−1.000	0.317
	MISS-DWI	44	9	0	83.0		
Contrast	CTD-DWI	44	9	0	83.0	−1.000	0.317
	MISS-DWI	45	8	0	84.9		
Deformation	CTD-DWI	39	13	1	73.6	−1.000	0.317
	MISS-DWI	38	14	1	71.7		
Artifact	CTD-DWI	23	30	0	43.4	−1.414	0.517
	MISS-DWI	22	30	1	41.5		

CTD: conventional 2D T2WI and 2D DWI; MISS: multiple instantaneous switchable scan; T2WI: T2-weighted imaging; DWI: diffusion-weighted imaging

showed that the PI-RADS scores assigned according to CTD and MISS were within the limits of agreement (mean difference±1.96 times the standard deviation of the differences), except for two cases.

The PI-RADS scores based on CTD and MISS had similar diagnostic abilities (area under curve [AUC] = 0.828 and 0.854) for predicting the presence of clinically significant PCa. The sensitivity and specificity of the PI-RADS scores were the same, whether based on MISS or CTD (sensitivity = 0.917 and specificity = 0.750). A PI-RADS score ≥4 was the imaging diagnostic standard for clinically significant PCa.

Reported preference for image interpretation
Reader 1 preferred to use MISS for image interpretation in 41.5% (22/53) of cases and had no preference for the other 58.5% (31/53)

of cases. Reader 2 preferred to use MISS for image interpretation in 47.2% (25/53) of cases and had no preference for the other 52.8% (28/53) of cases.

DISCUSSION
In this study, patients with a prostate lesion were scanned with both a MISS sequence and conventional sequences, to allow evaluation and comparisons between the techniques. Three-dimensional T2WI was reformatted in three orientations as axial, sagittal, and coronal images for lesion detection and characterization. The readers judged that the delineation of the fine structure of seminal vesicles and prostate lesion contrast were better on 3D T2WI from the MISS acquisition than on the conventional acquisition.

Table 5: Structure delineation and image quality comparison between CTD-diffusion-weighted imaging and multiple instantaneous switchable scan-diffusion-weighted imaging by reader 2

Content	Sequences	Score of 3	Score of 2	Score of 1	Ratio of clearly structure delineation (%)	Z	P
Delineation of structure							
Zonal anatomy	CTD-DWI	49	4	0	92.5	−1.000	0.317
	MISS-DWI	50	3	0	94.3		
Prostate capsule	CTD-DWI	48	5	0	90.6	−1.000	0.317
	MISS-DWI	50	3	0	94.3		
Nerve vascular bundle	CTD-DWI	43	10	0	84.9	−1.000	0.317
	MISS-DWI	43	9	1	81.1		
Seminal vesicles	CTD-DWI	43	10	0	84.9	−1.000	0.317
	MISS-DWI	43	9	1	81.1		
Image quality							
Sharpness	CTD-DWI	47	6	0	88.7	0	1.000
	MISS-DWI	47	6	0	88.7		
Contrast	CTD-DWI	44	9	0	83.0	0	1.000
	MISS-DWI	44	9	0	83.0		
Deformation	CTD-DWI	47	6	0	88.7	−0.333	0.739
	MISS-DWI	45	7	1	84.9		
Artifact	CTD-DWI	41	12	0	77.4	−1.000	0.317
	MISS-DWI	40	13	0	75.5		

CTD: conventional 2D T2WI and 2D DWI; MISS: multiple instantaneous switchable scan; T2WI: T2-weighted imaging; DWI: diffusion-weighted imaging

Overall, the MISS and CTD acquisitions were shown to have the same diagnostic accuracy.

According to PI-RADS v2, DWI is the dominant sequence for the diagnosis of PCa in the PZ, while T2WI is the best for evaluating cancer in the TZ.[15] DCE-MRI has a secondary role to T2WI and DWI, and it is often difficult to differentiate focal enhancement of small PCa, especially in the TZ.[5] Previous publications have shown images including axial, sagittal, and coronal T2WI, axial T1WI, and DWI series with ADC maps and have shown that the assigned DWI and T2WI scores can be sufficient for the stratification of patients for further diagnostic workup.[6,16] Hoeks *et al.*[17] concluded that the cancer detection and localization accuracy of biparametric MRI (AUC = 0.81) for high-grade PCa in the TZ was not inferior to that of mpMRI (AUC = 0.84).

The MISS sequence took proximately 4 min and 30 s to acquire, saving 1 min and 30 s of acquisition time compared with the two CTD sequences. The MISS sequence is more efficient because of the interleaved scan design for the 3D T2WI and 2D DWI (**Figure 1**). The otherwise empty duration between the two repeated cycles of 3D T2WI scans is filled by a shot of the DWI scan; therefore, the 3D T2WI and 2D DWI data can be acquired simultaneously during one repetition time. Another advantage of MISS is that the 3D T2WI and DWI are acquired in the same scan location, with more accurate and effective lesion registration, which is especially important for the guidance of target biopsy and local treatment.[18,19]

The results of this study demonstrate that clearer seminal vesicle structures and a higher contrast ratio can be obtained on MISS 3D T2WI than on conventional 2D T2WI. The 3D T2WI sequence uses nonspatially selective refocusing pulses with short echo spacing to achieve extended echo trains and subsequent rapid acquisition of individual k-space planes and is termed "sampling perfection with application-optimized contrasts using different flip angle evolutions." This sequence has been proposed as a method for efficient acquisition of 3D T2WI data sets.[10,20] Mugler *et al.*[21] found it was feasible to use 3D T2WI to obtain volumetric data sets of the brain, while another study found the benefit of using 3D T2WI as a magnetic resonance cholangiopancreatography sequence, with improved bile duct visualization and reduced artifacts.[22] In our study, we demonstrate that 3D T2WI offered greater image contrast for PCa detection than 2D T2WI, echoing a recent publication from Rosenkrantz *et al.*[11] stating that 3D T2WI had significantly greater tumor-to-peripheral zone contrast. The higher contrast between lesion and background could help in the differentiation of PCa. Furthermore, compared with three orthogonal multislice T2WI acquisitions (axial, sagittal, and coronal planes, as is often performed in practice), 3D T2WI images may be reformatted in all orientations, as required for lesion detection and characterization, and obviously with a shorter acquisition time than three separate 2D sequences.

PI-RADS v2 emphasizes the concept of a dominant sequence (DWI for lesions in the PZ and T2WI for lesions in the TZ), with the relegation of DCE to a tie-breaker role when a lesion remains indeterminate on T2WI and DWI. In this study, T2WI and DWI were evaluated together for lesion characterization, without reference to DCE images. With regard to the Bland–Altman plots, the PI-RADS scores assigned from the CTD and MISS were within the limits of agreement (d − 1.96 s.d. and d + 1.96 s.d.), except for two cases, which means that there was no significant difference between PI-RADS based on CTD and MISS. The sensitivity and specificity for clinically significant cancer detection on MISS and CTD were the same, with both sequences exhibiting a high ability to predict the presence of clinically significant cancer. A previous study showed a similar result, in which a 3D T2-weighted sequence had the same level of diagnostic accuracy as a 2D turbo spin-echo (TSE) sequence for the detection of PCa, despite a substantial reduction in acquisition time.[11] Therefore, the diagnostic value of MISS should satisfy the clinical requirement.

There were several limitations to this study. First, according to the recommendation of PI-RADS v2, DWI scanning should employ high diffusion gradients, which may be helpful for highlighting index tumors of the prostate.[23] Therefore, MISS acquisitions with higher *b*-value (*b*: diffusion sensitivity coefficient) series should be tested; these may have a higher clinical value not only simplifying the scanning process but also providing more valuable data. Second, the lack of

histopathology for many patients may have been a cause of bias. More histopathology results should be included in further research.

CONCLUSION

With reduced acquisition time, better lesion display, and higher contrast ratio, simultaneous acquisition of 3D T2WI and DWI of the prostate gland is feasible on 3T MRI and shows comparable diagnostic performance to conventional scanning sequences.

AUTHOR CONTRIBUTIONS

YL, WW, XBQ, HHW, and XYW planned, coordinated, and conducted the study. YL, WW, and GG analyzed the data and performed the statistical study. YL and XYW wrote and revised the manuscript. XDZ and XYW supervised the project. All authors read and approved the final manuscript.

COMPETING INTERESTS

All authors declare no competing interests.

REFERENCES

1   Heijmink SW, Fütterer JJ, Strum SS, Oyen WJ, Frauscher F, *et al*. State-of-the-art uroradiologic imaging in the diagnosis of prostate cancer. *Acta Oncol* 2011; 50: 25–38.
2   Kirkham AP, Emberton M, Allen C. How good is MRI at detecting and characterising cancer within the prostate? *Eur Urol* 2006; 50: 1163–75.
3   Barentsz JO, Weinreb JC, Verma S, Thoeny HC, Tempany CM, *et al*. Synopsis of the PI-RADS v2 guidelines for multiparametric prostate magnetic resonance imaging and recommendations for use. *Eur Urol* 2016; 69: 41–9.
4   Weinreb JC, Barentsz JO, Choyke PL, Cornud F, Haider MA, *et al*. PI-RADS prostate imaging-reporting and data system: 2015, version 2. *Eur Urol* 2016; 69: 16–40.
5   Monni F, Fontanella P, Grasso A, Wiklund P, Ou YC, *et al*. Magnetic resonance imaging in prostate cancer detection and management: a systematic review. *Minerva Urol Nefrol* 2017; 69: 567–78.
6   Scialpi M, Falcone G, Scialpi P, D'Andrea A. Biparametric MRI: a further improvement to PIRADS 2.0? *Diagn Interv Radiol* 2016; 22: 297–8.
7   de Bruin PW, Koken P, Versluis MJ, Aussenhofer SA, Meulenbelt I, *et al*. Time-efficient interleaved human (23)Na and (1)H data acquisition at 7 T. *NMR Biomed* 2015; 28: 1228–35.
8   Henningsson M, Mens G, Koken P, Smink J, Botnar RM. A new framework for interleaved scanning in cardiovascular MR: application to image-based respiratory motion correction in coronary MR angiography. *Magn Reson Med* 2015; 73: 692–6.
9   Mottet N, Bellmunt J, Briers E, Bolla M, Bourke P, *et al*. European Association of Urology. Guidelines on prostate cancer. European Association of Urology, update 6.7.2.3; March, 2015. Available from: http://www.uroweb.org/guideline/prostate-cancer/. [Last accessed on 2015 Jul 17].
10   Kim T, Murakami T, Hori M, Onishi H, Tomoda K, *et al*. Effect of superparamagnetic iron oxide on tumor-to-liver contrast T2*-weighted gradient-echo MRI: comparison between 3.0T and 1.5T MR systems. *J Magn Reson Imaging* 2009; 29: 595–600.
11   Rosenkrantz AB, Neil J, Kong X, Melamed J, Babb JS, *et al*. Prostate cancer: comparison of 3D T2-weighted with conventional 2D-weighted imaging for image quality and tumor detection. *AJR Am J Roentgenol* 2010; 194: 446–52.
12   Xia Y, Guan Y, Fan L, Liu SY, Yu H, *et al*. Dynamic contrast enhanced magnetic resonance perfusion imaging in high-risk smokers and smoking-related COPD: correlations with pulmonary function tests and quantitative computed tomography. *COPD* 2014; 11: 510–20.
13   Kuhl CK, Gieseke J, von Falkenhausen M, Textor J, Gernert S, *et al*. Sensitivity encoding for diffusion-weighted MR imaging at 3.0T: intraindividual comparative study. *Radiology* 2005; 234: 517–26.
14   Polanec S, Helbich TH, Bickel H, Pinker-Domenig K, Georg D, *et al*. Head-to-head comparison of PI-RADS v2 and PI-RADS v1. *Eur J Radiol* 2016; 85: 1125–31.
15   Rosenkrantz AB, Babb JS, Taneja SS, Ream JM. Proposed adjustments to PI-RADS version 2 decision rules: impact on prostate cancer detection. *Radiology* 2016; 283: 119–29.
16   Radtke JP, Boxler S, Kuru TH, Wolf MB, Alt CD, *et al*. Improved detection of anterior fibromuscular stroma and transition zone prostate cancer using biparametric and multiparametric MRI with MRI-targeted biopsy and MRI-US fusion guidance. *Prostate Cancer Prostatic Dis* 2015; 18: 288–96.
17   Hoeks CM, Hambrock T, Yakar D, Hulsbergen-van de Kaa CA, Feuth T, *et al*. Transition zone prostate cancer: detection and localization with 3-T multiparametric MR imaging. *Radiology* 2013; 266: 207–17.
18   Tao JX, Hawes-Ebersole S, Baldwin M, Shah S, Erickson RK, *et al*. The accuracy and reliability of 3D CT/MRI co-registration in planning epilepsy surgery. *Clin Neurophysiol* 2009; 120: 748–53.
19   Nicola LR, Mark E, Caroline MM. MRI-targeted prostate biopsy: a review of technique and results. *Nat Rev Urol* 2013; 10: 589–97.
20   Cornfeld DM, Israel G, McCarthy SM, Weinreb JC. Pelvic imaging using a T1W fat-suppressed three-dimensional dual echo Dixon technique at 3T. *J Magn Reson Imaging* 2008; 28: 121–7.
21   Mugler JP 3rd, Bao S, Mulkern RV, Guttmann CR, Robertson RL, *et al*. Optimized single-slab three-dimensional spin-echo MR imaging of the brain. *Radiology* 2000; 216: 891–9.
22   Haystead CM, Dale BM, Merkle EM. N/2 ghosting artifacts: elimination at 3.0-T MR cholangiography with SPACE pulse sequence. *Radiology* 2008; 246: 589–95.
23   Rosenkrantz AB, Hindman N, Lim RP, Das K, Babb JS, *et al*. Diffusion-weighted imaging of the prostate: comparison of b1000 and b2000 image sets for index lesion detection. *J Magn Reson Imaging* 2013; 38: 694–700.